NASA Technical Memorandum 4053

Nucleon-Nucleus Interaction Data Base: Total Nuclear and Absorption Cross Sections

J. W. Wilson, L. W. Townsend, W. W. Buck,
S. Y. Chun, B. S. Hong, and S. L. Lamkin

AUGUST 1988

NASA

NASA Technical Memorandum 4053

Nucleon-Nucleus Interaction Data Base: Total Nuclear and Absorption Cross Sections

J. W. Wilson and L. W. Townsend
Langley Research Center
Hampton, Virginia

W. W. Buck, S. Y. Chun, and B. S. Hong
Hampton University
Hampton, Virginia

S. L. Lamkin
Planning Research Corporation
Hampton, Virginia

Abstract

Neutron total cross sections are represented for Li to Pu targets at energies above 0.1 MeV and less than 100 MeV using a modified nuclear Ramsauer formalism. The formalism is derived for energies above 100 MeV by fitting theoretical cross sections. Neutron absorption cross sections are represented by analytic expressions of similar form, but shape resonance phenomena of the Ramsauer effect are not present. Elastic differential cross sections are given as a renormalized impulse approximation. These cross section data bases will be useful for nucleon transport applications.

1. Introduction

In an earlier report (ref. 1), we presented a relatively complete transport code for high energy nucleons. The data base for that code was complete but somewhat inaccurate. The present report describes the further development of the data base by improving the total nuclear cross sections (σ_{tot}) and the nuclear absorption cross sections (σ_{abs}). The effects of this improvement on the elastic scattered neutron differential cross sections (σ_s) are also presented.

2. Total Nuclear Cross Sections

After many decades of experimental activity at various accelerators with ever-increasing energies, the cross sections for two-nucleon interactions are reasonably well defined. Although recent advances in the theory of the two-nucleon interaction in terms of phenomenological meson exchange models (ref. 2) show considerable success, a simple parameterization of the experimental data is sufficient for our purposes. For energy $E \geq 25$ MeV, the proton-proton (pp) total cross section is found to be reasonably approximated by

$$\sigma_{pp}(E) = (1 + 5/E)\{40 + 109 \, \cos(0.199 \, \sqrt{E})$$
$$\times \exp[-0.451(E - 25)^{0.258}]\} \quad (2.1)$$

and for lower energies

$$\sigma_{pp}(E) = \exp\{6.51 \, \exp[-(E/134)^{0.7}]\} \quad (2.2)$$

These forms are shown in comparison with experimental data (ref. 3) in figure 1. For $E \geq 0.1$ MeV, the neutron-proton (np) cross section is taken as

$$\sigma_{np}(E) = 38 \; + \; 12\,500 \, \exp[-1.187(E - 0.1)^{0.35}] \quad (2.3)$$

and at lower energies

$$\sigma_{np}(E) = 26\,000 \, \exp[-(E/0.282)^{0.3}] \quad (2.4)$$

These forms are shown in comparison with experimental data (ref. 3) in figure 2.

The low energy neutron-nucleus total cross sections exhibit a complicated fine resonance structure over a broad, slowly varying background. This background is marked by very broad Ramsauer resonances that persist even to neutron energies of 100 MeV. Although a simple fundamental theory for the Ramsauer resonances is not available, a semi-empirical formalism is given by Angeli and Csikai (refs. 4 and 5). Their formalism starts with the usual partial wave expansion as

$$\sigma_{tot} = 2\pi\lambda^2 \sum_{\ell} (2\ell + 1)[1 - \text{Re}(n_\ell)] \quad (2.5)$$

where $\text{Re}(Z)$ denotes real part of Z with

$$n_\ell = \exp(i\delta_\ell) \quad (2.6)$$

where δ_ℓ is the complex phase shift for the ℓth partial wave and $i = \sqrt{-1}$. In the opaque nucleus model, $n_\ell \approx 1$ for all $\ell > R/\lambda$, where R is the nuclear radius, which leads Angeli and Csikai to assume

$$\sigma_{tot} \approx 2\pi(R + \lambda)^2[1 - \text{Re}(\eta)] \quad (2.7)$$

where $\eta = 0$ gives the usual opaque nucleus result such that

$$\text{Re}(\eta) = e^{-\text{Im}(\delta)} \, \cos[\text{Re}(\delta)] \equiv p \, \cos(qA_t^{1/3} - r) \quad (2.8)$$

where A_t is the mass number of the target nucleus, is a reasonable starting point to parameterize the total cross sections. Their complete parameterization is

$$\sigma_{tot} = 2\pi(r_o A_t^{1/3} + \lambda)^2[a - p \, \cos(qA_t^{1/3} - r)] \quad (2.9)$$

where $r_o = 1.4$ fm, and the neutron wavelength is

$$\lambda = \frac{4.55}{\sqrt{E}} \frac{A_t + 1}{A_t} \quad (2.10)$$

The parameters of Angeli and Csikai are adequately approximated by

$$a = \frac{1}{1 + 2/(3.8E + 0.1E\sqrt{E} + 0.1E^3\sqrt{E})} \quad (2.11)$$

$$p = 0.15 - 0.0066\sqrt{E} \quad (2.12)$$

$$q = 2.72 - 0.203\sqrt{E} \quad (2.13)$$

$$r = \min\{-5.3 + 1.66\sqrt{E}, \; 1.3\} \quad (2.14)$$

Strictly speaking, equations (2.9) to (2.14) apply only to $A_t \geq 40$ and $0.5 \leq E \leq 40$ MeV. A simple extension to all A_t and $0.1 \leq E \leq 100$ MeV gives qualitatively similar results to the experimental data and provides a starting point for representing the total cross section. The cross sections given by equations (2.9) to (2.14) are shown in figure 3. This should be compared with the experimental data (ref. 6) shown in figure 4. Note the data in figure 4 have only the broad resonances shown. The very narrow resonances have been averaged. We now seek some modification to the Angeli-Csikai cross sections to better approximate the total cross sections.

Our modifications to the Angeli-Csikai formalism are as follows:

(1) If $A_t > 75$, then a is taken as 0.18 for values of equation (2.11) less than 0.18.

(2) The value of p is taken to be greater than $0.4a$ unless $A_t > 76$, for which p can be as small as $0.3a$.

(3) A modifying factor of

$$1 + D \exp(-\alpha E)$$

is used with

$$D = \begin{cases} 0.5 & (145 < A_t < 235) \\ 1.0 & \text{(Otherwise)} \end{cases}$$

and

$$\alpha = \begin{cases} 1.0 & (205 < A_t < 235) \\ 2.0 & \text{(Otherwise)} \end{cases}$$

(4) An additional modifying factor is applied as

$$F_1 \Big\{ 1 - 0.5 \, \exp[-(A_t - 63.54)^2/20]$$
$$- 0.45 \exp[-(A_t - 58.71)^2/4] \, \exp(-2E) + F_2 \Big\}$$

where

$$F_1 = \begin{cases} 0.7 & (A_t \leq 63, E \leq 0.8) \\ 1.0 & \text{(Otherwise)} \end{cases}$$

$$F_2 = \begin{cases} 0 & (E > 0.5) \\ -4.95 \, \exp(-18E) & (40 \leq A_t < 42) \\ -1.79 \, \exp(-15E) & (32 \leq A_t < 34) \end{cases}$$

(5) If $A_t < 30$, then numerical interpolation between experimental values is used.

The final cross sections as modified above are shown in figure 5 and should be compared with figure 4.

The total cross sections above 100 MeV have been taken from reference 7. The high energy cross sections of reference 7 have been approximated by

$$\sigma_{\text{tot}}(A_t, E) = 52.5 A_t^{0.758} \Big[1 + (0.8 + 2.4 \, e^{-A_t/30})$$
$$\times \, e^{-E/135} \sin \theta_E \Big] \qquad (2.15)$$

where the phase angle is given by

$$\theta_E = \begin{cases} 14.41 & (E \leq 40 \text{ MeV}) \\ 1.29 \ln^2(E) - \pi & (E > 40 \text{ MeV}) \end{cases} \qquad (2.16)$$

In figures 6 to 9, the expressions (2.15) and (2.16) are shown in comparison with the theory of Townsend and Wilson (ref. 7) and a compilation of experiments. As can be seen in these figures, equations (2.15) and (2.16) give reasonable fits above 100 MeV. Equations (2.9) to (2.14) are connected smoothly at 70 MeV to the results of equations (2.15) and (2.16) at 130 MeV with an assumed exponential dependence on energy. The total cross section is used to calculate the scattering cross section as

$$\sigma_s(E) = \sigma_{\text{tot}}(E) - \sigma_{\text{abs}}(E) \qquad (2.17)$$

The total neutron-nucleus cross section is shown in comparison with experimental data (ref. 6) in figures 10 to 13 (experimental data shown as the dashed curve). Also shown are the cross sections (dot-dash curve listed as "Prior") used in reference 1. Clearly the present result is a great improvement.

3. Nuclear Absorption Cross Sections

Qualitatively, the nuclear absorption cross sections show an energy dependence similar to that observed for the total nuclear cross sections. An analytic formula for protons was derived by Letaw et al. (ref. 8) by first fitting the cross sections of Bobchenko et al. (ref. 9) with the formula

$$\sigma_{A_{\text{tot}}} = 45 A_t^{0.7} \{ 1 + 0.016 \, \sin[5.3 - 2.63 \ln(A_t)] \} \qquad (3.1)$$

Equation (3.1) reproduces the Bobchenko data to within 2 percent (ref. 8). A somewhat better fit to the Bobchenko data is given by

$$\sigma_{A_T} = 45 A_t^{0.7} (1 - 0.018 \sin \theta_{A_t}) \qquad (3.2)$$

2

where the angle θ_{A_t} is

$$\theta_{A_t} = 2.94 \ln(A_t) + 0.63 \sin[3.92 \ln(A_t) - 2.329] - 0.176 \tag{3.3}$$

Equation (3.2) fits the Bobchenko data to within the 1.2-percent difference that is on the order of the experimental uncertainty (ref. 9). Although the Bobchenko data represent a consistent set of measurements for many different targets and probably define well the A_t dependence of the high energy cross sections, they may nonetheless be in error in absolute value, as suggested by many other independent experiments (refs. 10 and 11).

Letaw et al. assume the energy dependence for all nuclei to be the same and approximated by

$$f(E) = 1 - 0.62 \exp(-E/200) \sin(10.9E^{-0.28}) \tag{3.4}$$

where the nucleon kinetic energy is in units of MeV. We observe oscillations according to the quantum-mechanical calculations of Townsend and Wilson (ref. 10) with phase angle

$$\theta_E = \left\{ \begin{array}{ll} 1.44 & (E < 25 \text{ MeV}) \\ 1.33 \ln(E) - 2.84 & (\text{Otherwise}) \end{array} \right\} \tag{3.5}$$

but with an A_t-dependent amplitude given by

$$f(E) = 1 - (0.3E^{-0.22} + 0.76e^{-E/135})$$
$$(0.4 + 0.9e^{-A_t/30}) \sin \theta_E \tag{3.6}$$

In figures 14 to 18, the absorption cross sections as given by equations (3.3), (3.5), and (3.6) are shown in comparison with the fit of Letaw et al. and experiments. As one can see from the figures, it is difficult to assign a figure of merit to the fit, since great scatter in the experiments obscures the result. Generally, above 20 MeV the results are on the order of 10 percent accurate as estimated from the scatter in the experiments.

Below 20 MeV, the neutron cross sections are represented by numerical data sets at discrete energies of 1, 3, 5, 10, 14, and 20 MeV as taken from references 6, 11, and 12. These are shown in figures 19 to 24. Intermediate energy values are found according to

$$\sigma(A_t, E) = \sigma(A_t, E_i) \, e^{-a(E-E_i)} \tag{3.7}$$

where E_i and a are taken according to the appropriate subinterval. The cross sections are assumed to be zero at energies below 0.5 MeV. The absorption cross sections for elements from lithium to plutonium for energies between 1 and 100 MeV are displayed in figure 25.

4. Nucleon-Nucleus Elastic Spectrum

The nucleon-nucleus differential elastic cross section in the impulse (Chew) approximation (note, this is just the Born term of the optical model in ref. 13) is given by

$$\frac{d\sigma}{dq^2} = Ce^{-2bq^2}[F_{A_t}(q^2)]^2$$
$$\approx C'e^{-2bq^2 - 2a^2q^2/3} \tag{4.1}$$

where b is the slope parameter of the equation (see ref. 1) averaged among nuclear constituents, q is the magnitude of momentum transfer, a is the nuclear rms radius, and F_{A_t} is the nuclear form factor. The nuclear rms radius in terms of the rms charge radius in femtometers is given as

$$a = \sqrt{a_c^2 - 0.64} \tag{4.2}$$

where the rms charge radius is

$$a_c = \left\{ \begin{array}{ll} 0.84 & (A_t = 1) \\ 2.17 & (A_t = 2) \\ 1.78 & (A_t = 3) \\ 1.63 & (A_t = 4) \\ 2.4 & (6 \leq A_t \leq 14) \\ 0.82A_t^{1/3} + 0.58 & (A_t \geq 16) \end{array} \right\} \tag{4.3}$$

The nuclear form factor is the Fourier transform of the nuclear matter distribution. Note that equation (4.1) assumes the nuclear matter distribution is a Gaussian function, which is reasonable for the light mass nuclei but is less valid for $A_t \gg 20$.

The energy transferred to the nucleus, E_t, is restricted by kinematics to

$$0 \leq E_t \leq (1 - \alpha)E' \tag{4.4}$$

where

$$\alpha = \frac{(A_t - 1)^2}{(A_t + 1)^2} \tag{4.5}$$

The energy transfer spectrum is given as

$$f(E_t, E') = \frac{4A_t mc^2 \left(\frac{B+a^2}{3}\right) e^{-4A_t mc^2 \left(\frac{B+a^2}{3}\right)E_t}}{\left[1 - e^{-4A_t mc^2(1-\alpha)\left(\frac{B+a^2}{3}\right)E'}\right]} \tag{4.6}$$

3

where m is the nucleon mass and B is the interaction slope parameter. Similarly, the nucleon energy after scattering, E, is restricted to

$$\alpha E' \leq E \leq E' \tag{4.7}$$

The nucleon spectrum is given by

$$f(E, E') = \frac{4A_t mc^2 \left(\frac{B+a^2}{3}\right) e^{-4A_t mc^2 \left(\frac{B+a^2}{3}\right)(E'-E)}}{\left[1 - e^{-4A_t mc^2(1-\alpha)\left(\frac{B+a^2}{3}\right)E'}\right]} \tag{4.8}$$

One should note that both equations (4.6) and (4.8) reduce to the usual isotropic scattering result at low incident energy. The differential spectrum is normalized as

$$\frac{d\sigma_s}{dE} = \sigma_s(E') \, f(E, E') \tag{4.9}$$

where $\sigma_s(E')$ is the total scattering cross section obtained from equation (2.17).

The results of equation (4.9) are shown in comparison with experimental data (refs. 14 and 15) in figures 26 to 29. In these figures, θ_{cm} refers to the center-of-mass scattering angle while θ_{lab} is the corresponding angle in the laboratory. The comparison is rather good at the small angles, considering the simplicity of the present results. Also shown in the figures are results from reference 1 showing considerable improvement over the prior results. Much of the present discrepancy near forward scattering is due to errors in $\sigma_S(E)$ to which the present spectra are normalized in equation (4.9). At broader angles, the differences are due to the neglect of higher order corrections to the impulse term.

5. Concluding Remarks

The results reported herein are considerably more accurate than the results used in the original Langley Research Center transport code BRYNTRN. A version of BRYNTRN with these new data is now available.

NASA Langley Research Center
Hampton, Virginia 23665-5225
July 20, 1988

6. References

1. Wilson, John W.; Townsend, Lawrence W.; Chun, Sang Y.; Buck, Warren W.; Khan, Ferdous; and Cucinotta, Frank: *BRYNTRN: A Baryon Transport Computer Code—Computation Procedures and Data Base.* NASA TM-4037, 1988.

2. Gross, Franz: New Theory of Nuclear Forces—Relativistic Origin of the Repulsive Core. *Phys. Review D*, vol. 10, no. 1, July 1, 1974, pp. 223–242.

3. Lock, W. O.; and Measday, D. F.: *Intermediate Energy Nuclear Physics.* Methuen & Co. Ltd. (London), 1970.

4. Angeli, I.; and Csikai, J.: Total Neutron Cross Sections and the Nuclear Ramsauer Effect. *Nucl. Phys.*, vol. A158, no. 2, Dec. 14, 1970, pp. 389–392.

5. Angeli, I.; and Csikai, J.: Total Neutron Cross Sections and the Nuclear Ramsauer Effect. (II). $E_n = 0.5$–42 MeV. *Nucl. Phys.*, vol. A170, no. 3, Aug. 2, 1971, pp. 577–583.

6. Hughes, Donald J.; and Schwartz, Robert B.: *Neutron Cross Sections.* BNL 325, Second ed., Brookhaven National Lab., July 1, 1958.

7. Townsend, Lawrence W.; Wilson, John W.; and Bidasaria, Hari B.: *Nucleon and Deuteron Scattering Cross Sections From 25 MeV/Nucleon to 22.5 GeV/Nucleon.* NASA TM-84636, 1983.

8. Letaw, John R.; Silberberg, R.; and Tsao, C. H.: Proton-Nucleus Total Inelastic Cross Sections: An Empirical Formula for $E > 10$ MeV. *Astrophys. J.*, Suppl. ser., vol. 51, no. 3, Mar. 1983, pp. 271–276.

9. Bobchenko, B. M.; Buklei, A. E.; Vlasov, A. V.; Vorob'ev, I. I.; Vorob'ev, L. S.; Goryainov, N. A.; Grishuk, Yu. G.; Gushchin, O. B.; Druzhinin, B. L.; Zhurkin, V. V.; Zavrazhnov, G. N.; Kosov, M. V.; Leksin, G. A.; Stolin, V. L.; Surin, V. P.; Fedorov, V. B.; Fominykh, B. A.; Shvartsman, B. B.; Shevchenko, S. V.; and Shuvalov, S. M.: Measurement of Total Inelastic Cross Sections for Interaction of Protons With Nuclei in the Momentum Range From 5 to 9 GeV/c and for Interaction of π^- Mesons With Nuclei in the Momentum Range From 1.75 to 6.5 GeV/c. *Soviet J. Nucl. Phys.*, vol. 30, no. 6, Dec. 1979, pp. 805–813.

10. Townsend, Lawrence W.; and Wilson, John W.: *Tables of Nuclear Cross Sections for Galactic Cosmic Rays—Absorption Cross Sections.* NASA RP-1134, 1985.

11. Stehn, John R.; Goldberg, Murrey D.; Magurno, Benjamin A.; and Wiener-Chasman, Renate: *Neutron Cross Sections. Volume 1, $Z = 1$ to 20.* BNL 325, Second ed., Suppl. No. 2 (Physics—TID-4500, 32nd ed.), Sigma Center, Brookhaven National Lab. Associated Univ., Inc., May 1964.

12. Brodsky, Allen, ed.: *CRC Handbook of Radiation Measurement and Protection—General Scientific and Engineering Information, Volume I: Physical Science and Engineering Data.* CRC Press, Inc., c.1978.

13. Wilson, John W.; and Costner, Christopher M.: *Nucleon and Heavy-Ion Total and Absorption Cross Section for Selected Nuclei.* NASA TN D-8107, 1975.

14. Fernbach, S.: Nuclear Radii as Determined by Scattering of Neutrons. *Reviews Modern Phys.*, vol. 30, no. 2, pt. 1, Apr. 1958, pp. 414–418.

15. Goldberg, Murrey D.; May, Victoria M.; and Stehn, John R.: *Angular Distributions in Neutron-Induced Reactions. Volume I, $Z = 1$ to 22.* BNL 400, Second ed., Vol. I, Sigma Center, Brookhaven National Lab., Oct. 1962.
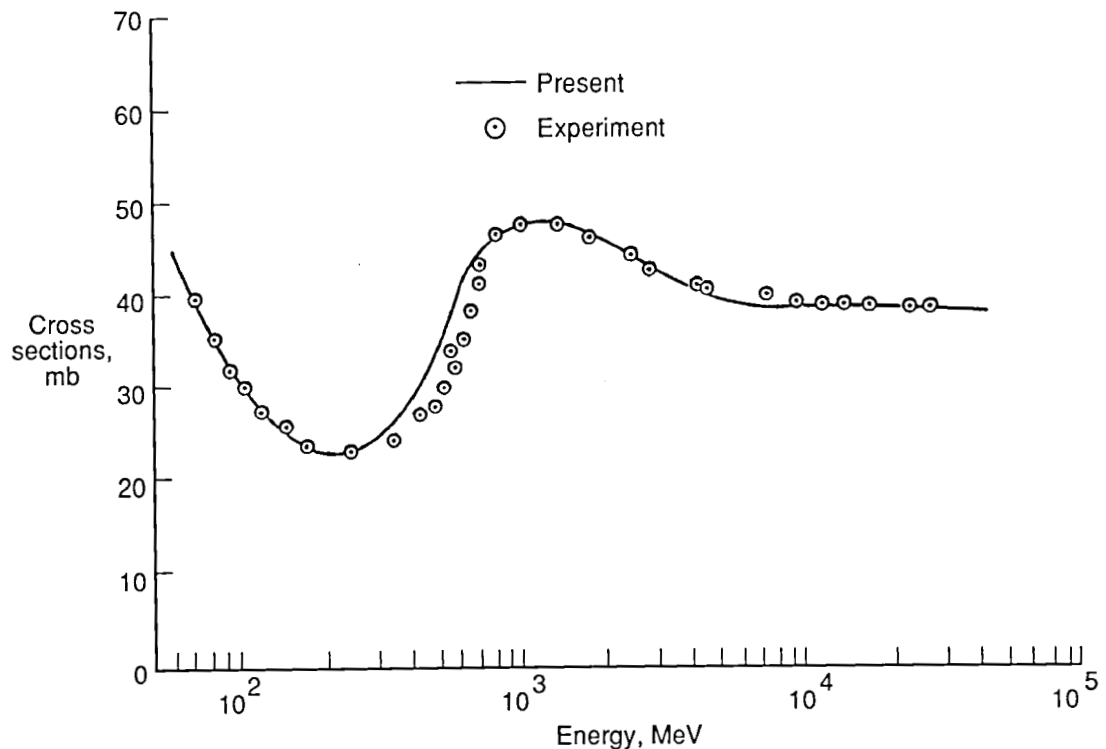
Figure 1. The total proton-proton cross sections according to the present formalism and various experiments.
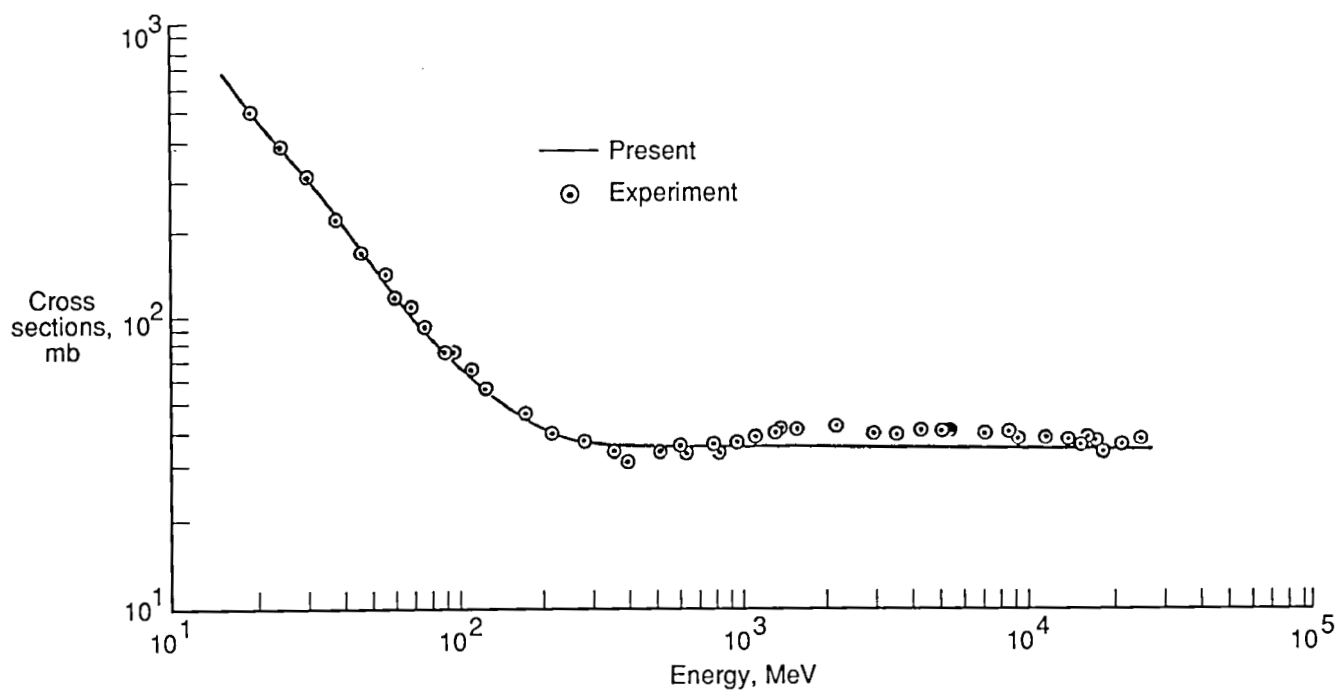

Figure 2. The total neutron-proton cross sections according to the present formalism and various experiments.
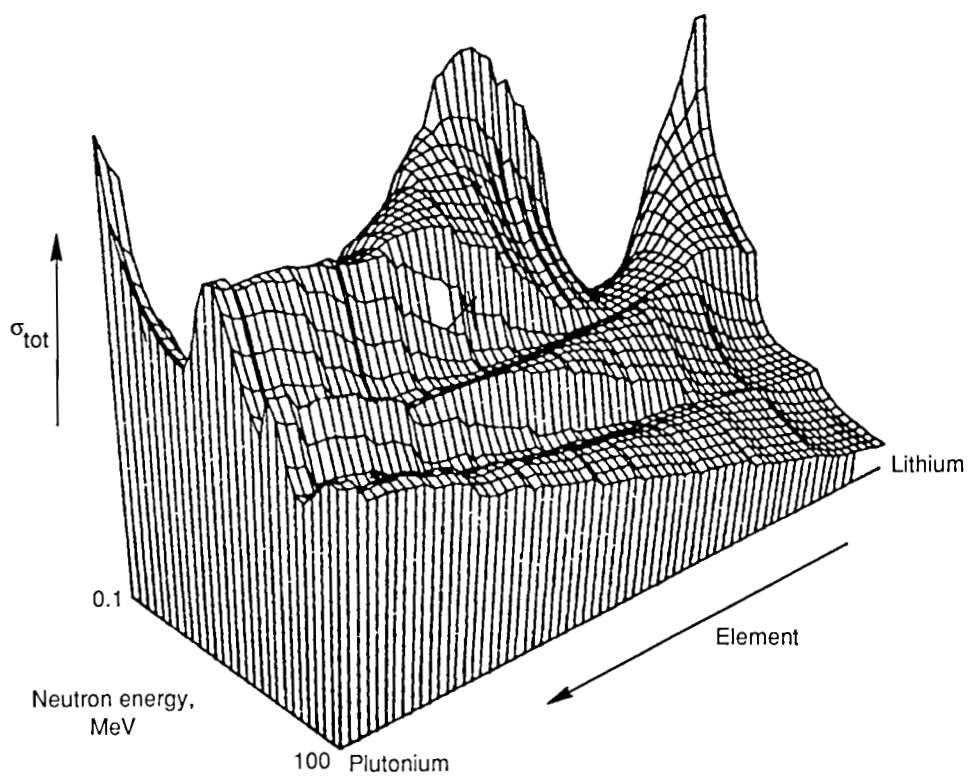
Figure 3. The total neutron-nucleus cross sections according to the Ramsauer resonance formalism.
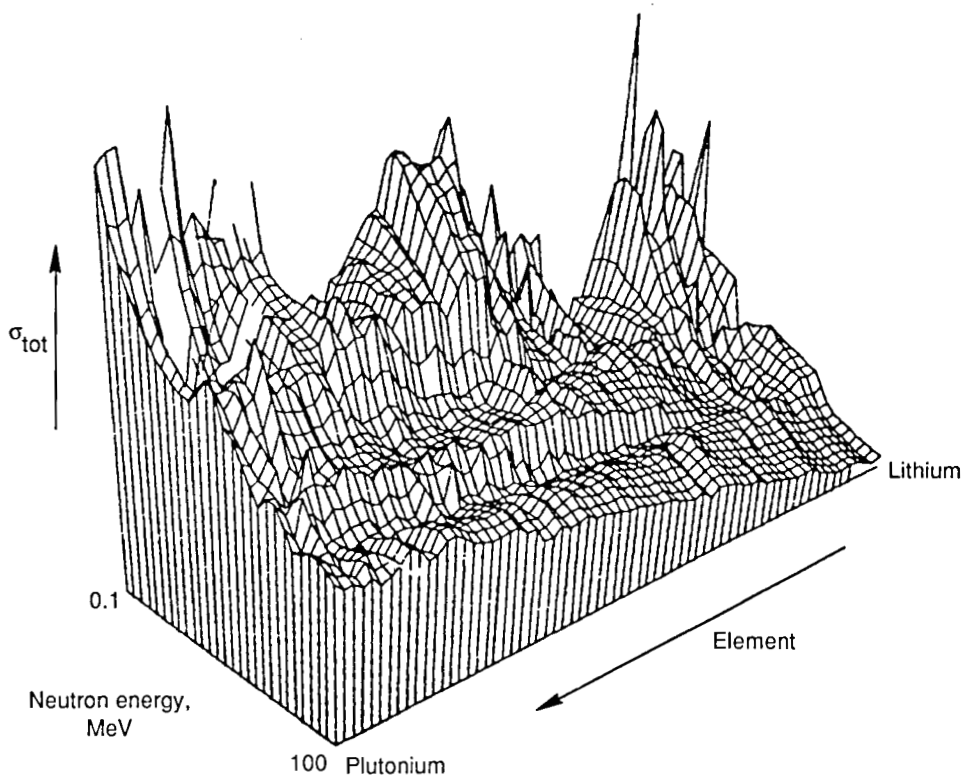

Figure 4. The total neutron cross sections according to reference 6.
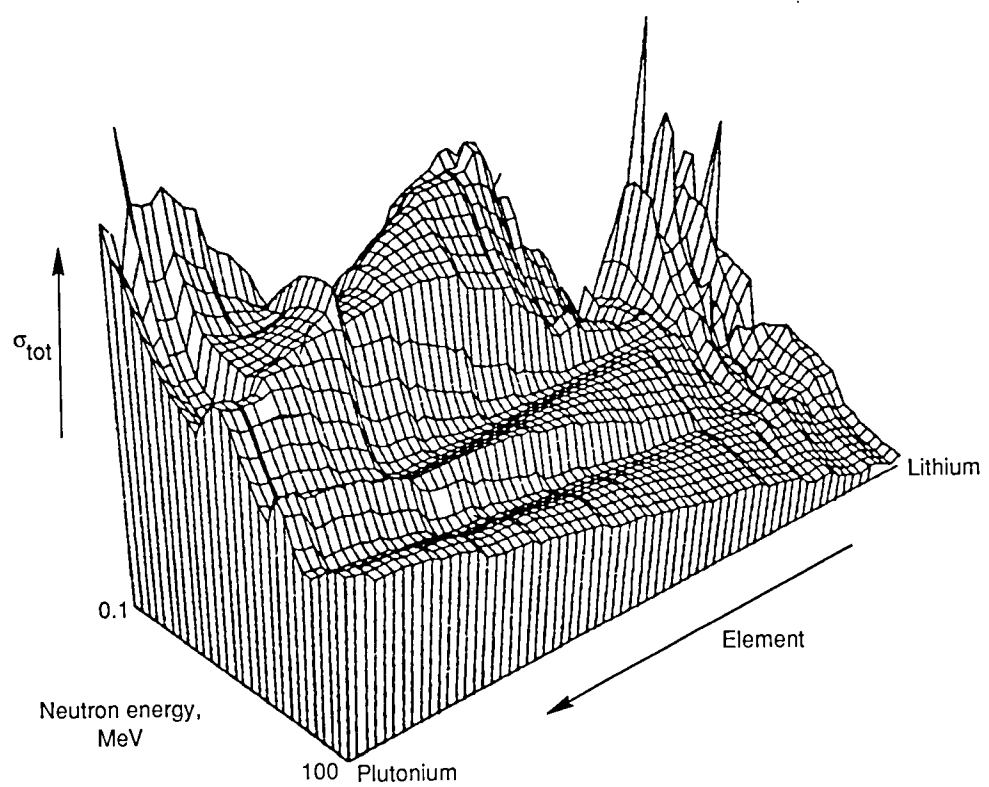
Figure 5. The total neutron-nucleus cross sections according to the present formalism.
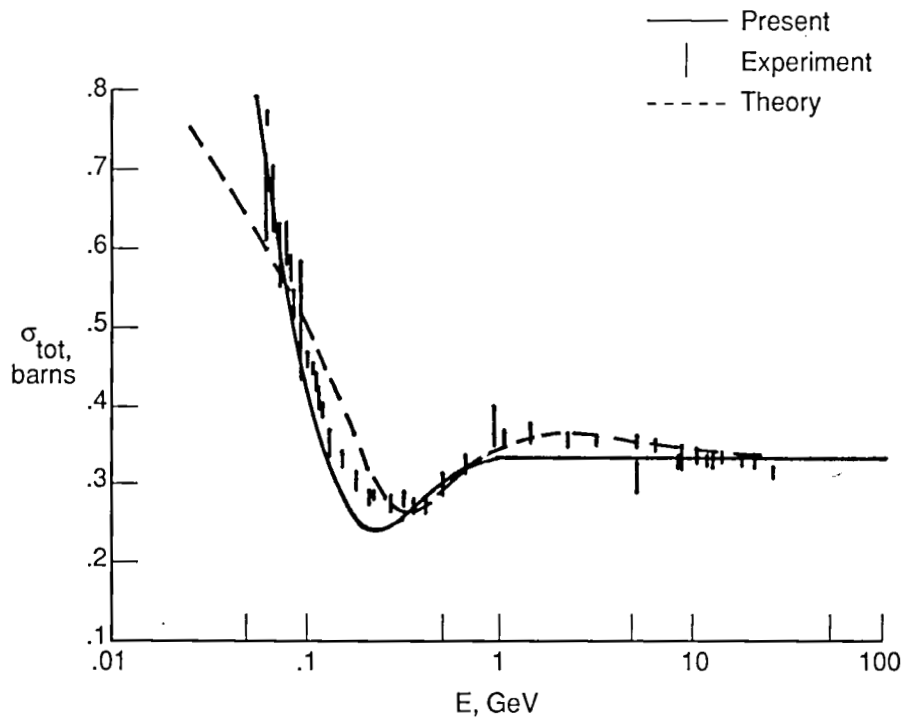
Figure 6. The total nucleon-carbon cross sections according to the present formalism, the theory of Townsend and Wilson, and various experiments.
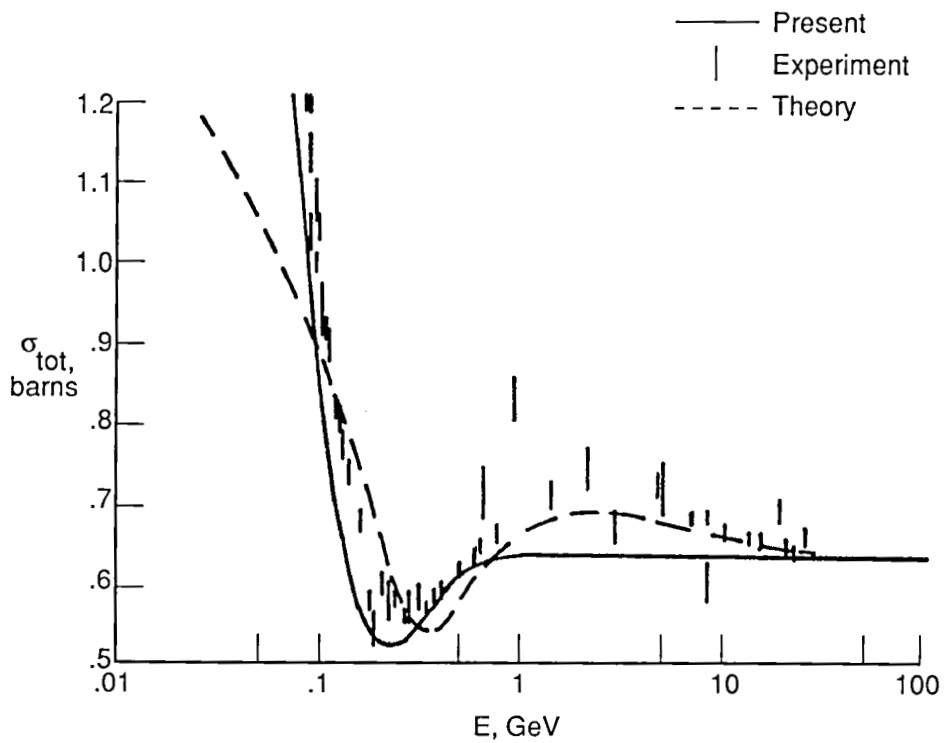
Figure 7. The total nucleon-aluminum cross sections according to the present formalism, the theory of Townsend and Wilson, and various experiments.
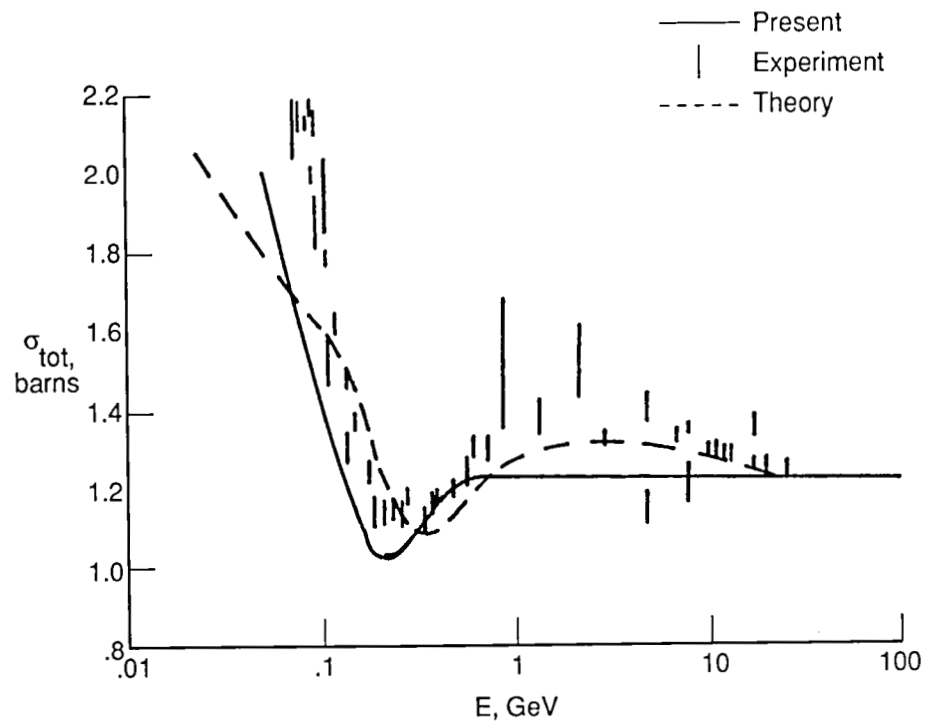
Figure 8. The total nucleon-copper cross sections according to the present formalism, the theory of Townsend and Wilson, and various experiments.
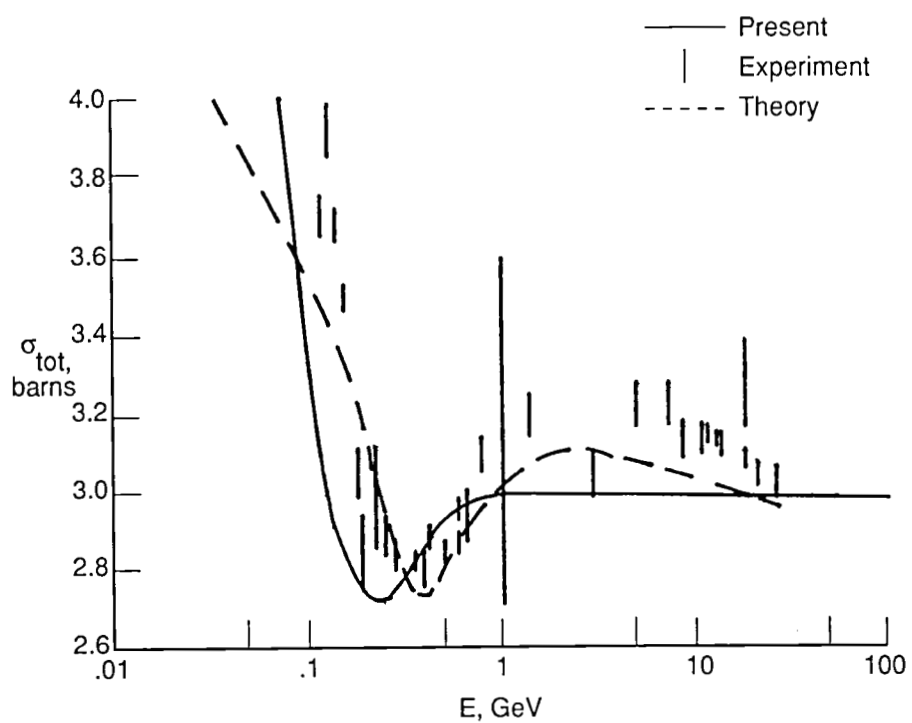
Figure 9. The total nucleon-lead cross sections according to the present formalism, the theory of Townsend and Wilson, and various experiments.
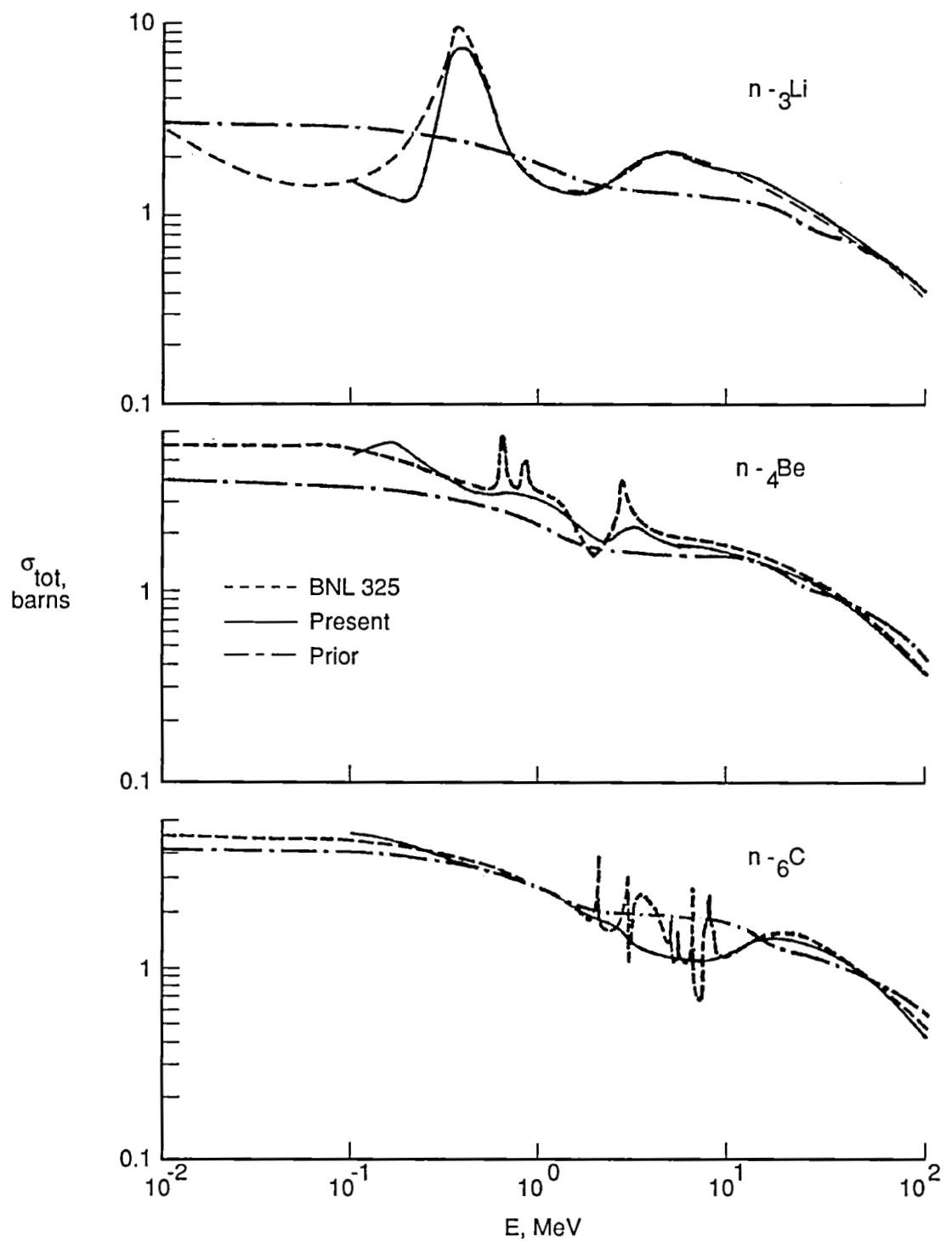
Figure 10. The total neutron-nucleus cross sections according to the prior data base (ref. 1), the present formalism, and an evaluated data base (ref. 6).
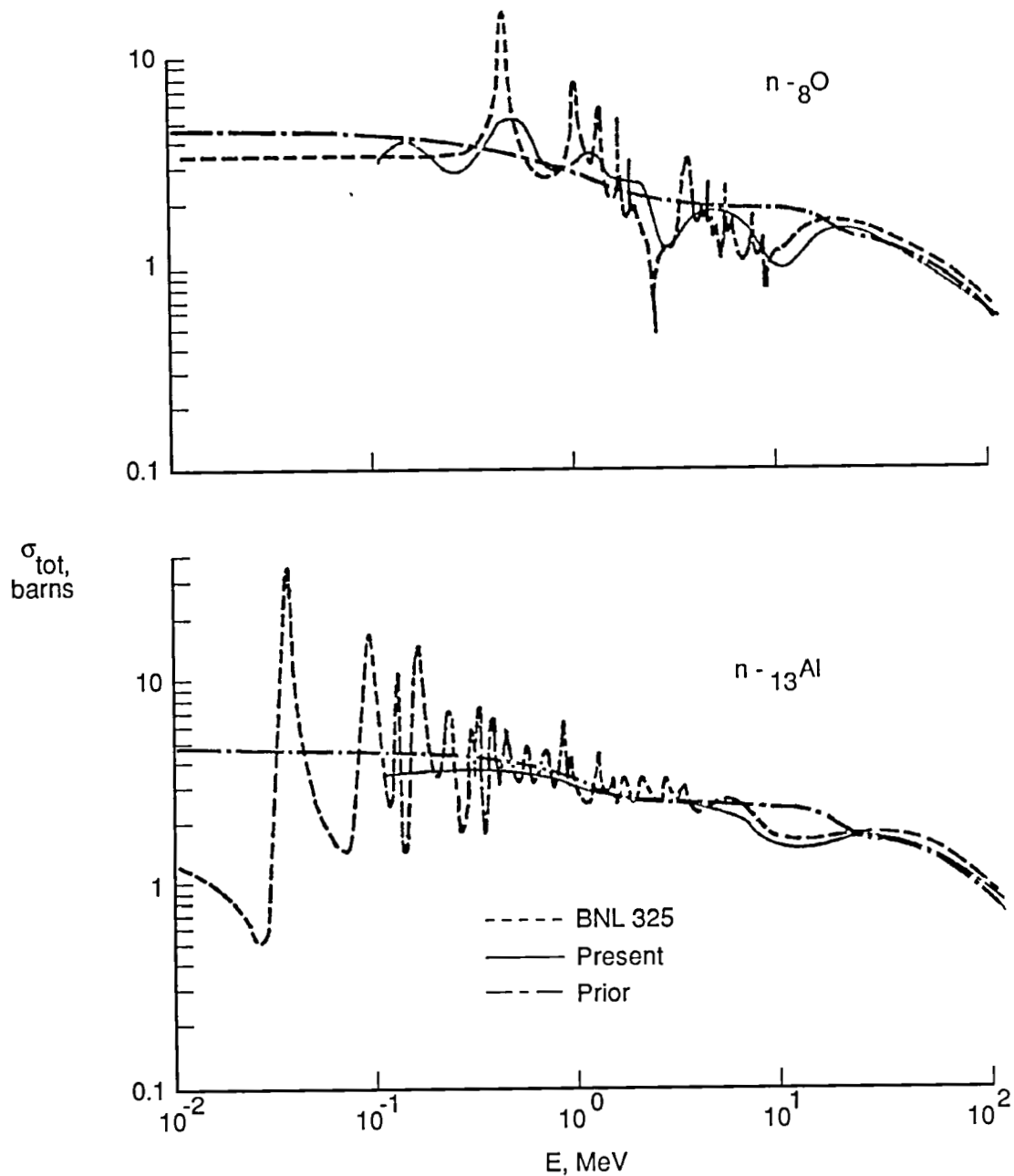
Figure 11. The total neutron-nucleus cross sections according to the prior data base (ref. 1), the present formalism, and an evaluated data base (ref. 6).
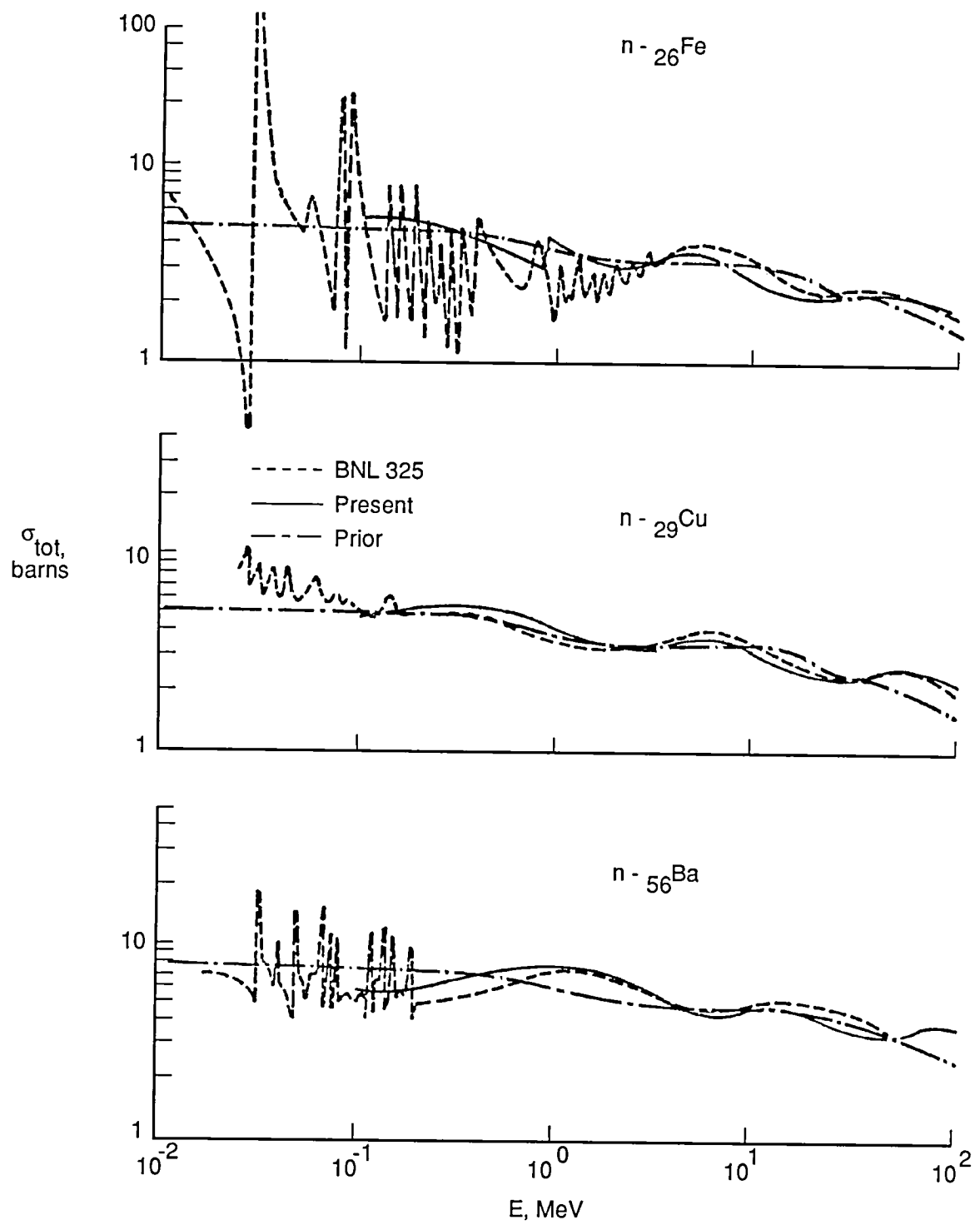
Figure 12. The total neutron-nucleus cross sections according to the prior data base (ref. 1), the present formalism, and an evaluated data base (ref. 6).
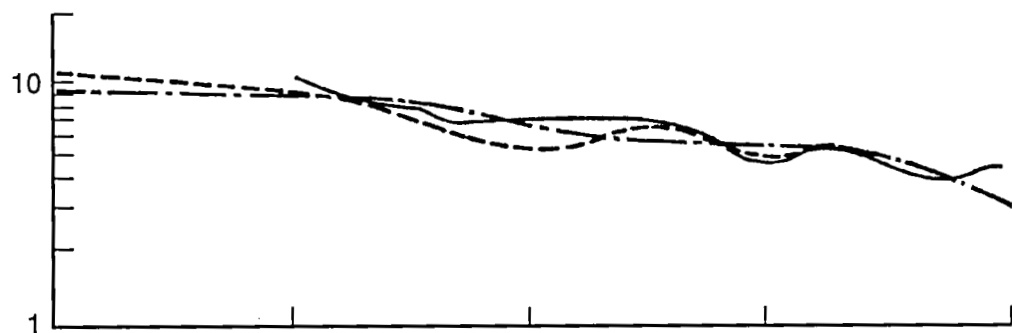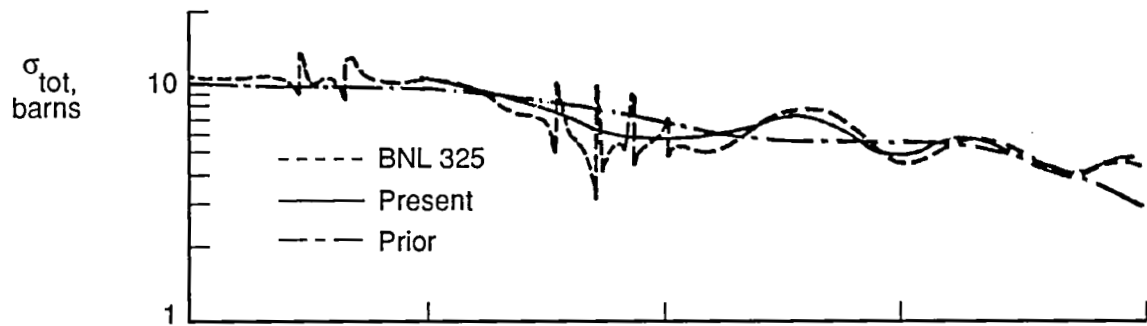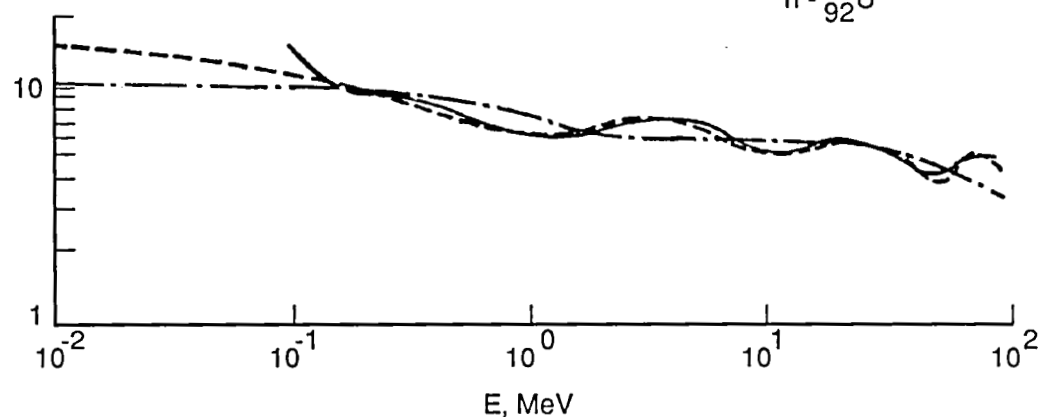
Figure 13. The total neutron-nucleus cross sections according to the prior data base (ref. 1), the present formalism, and an evaluated data base (ref. 6).
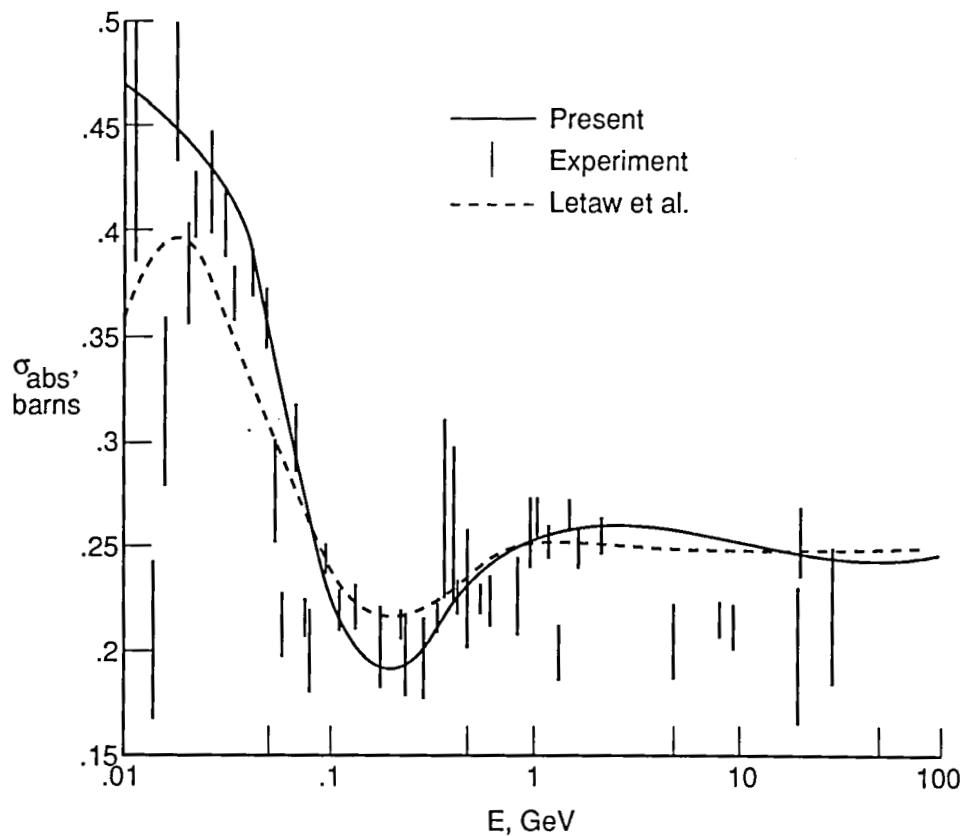
Figure 14. The neutron-carbon absorption cross sections according to the present formalism, Letaw et al. (ref. 8), and various experiments.
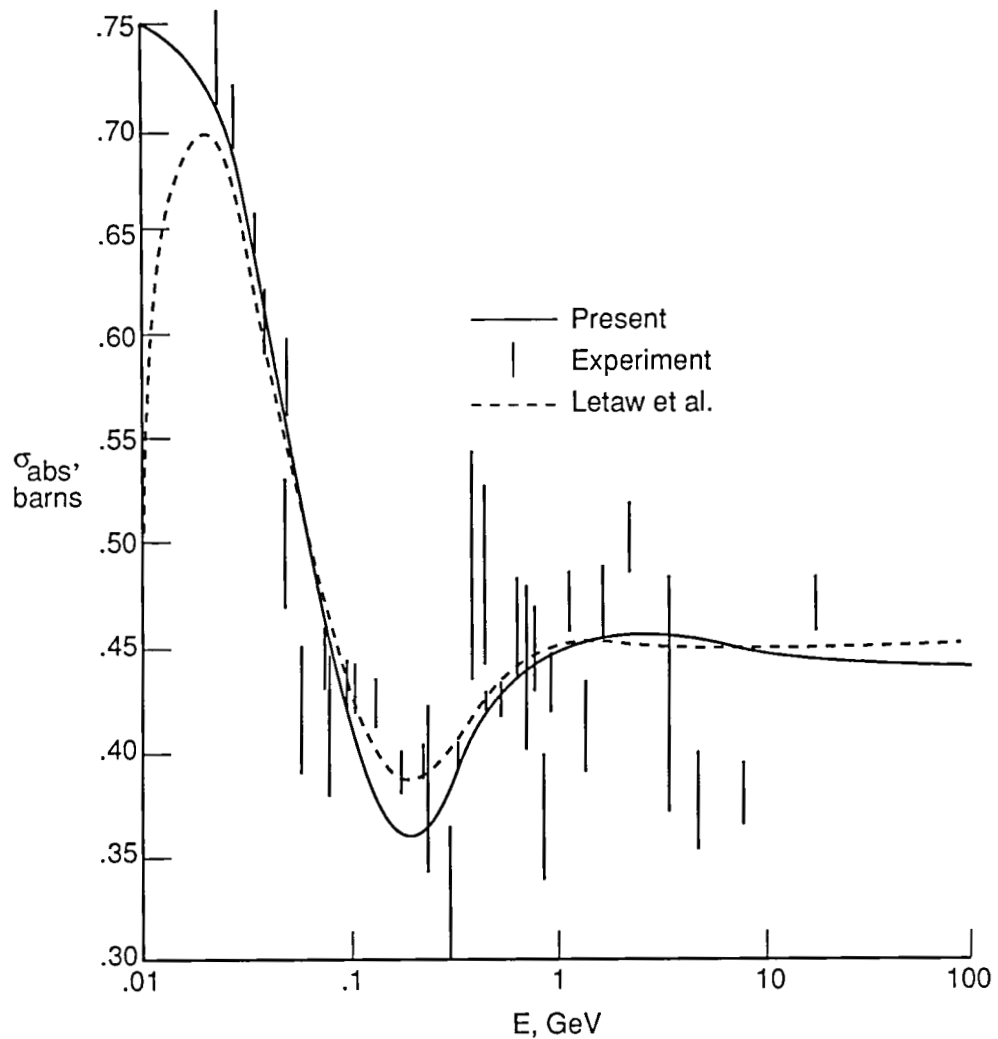
Figure 15. The neutron-aluminum absorption cross sections according to the present formalism, Letaw et al. (ref. 8), and various experiments.
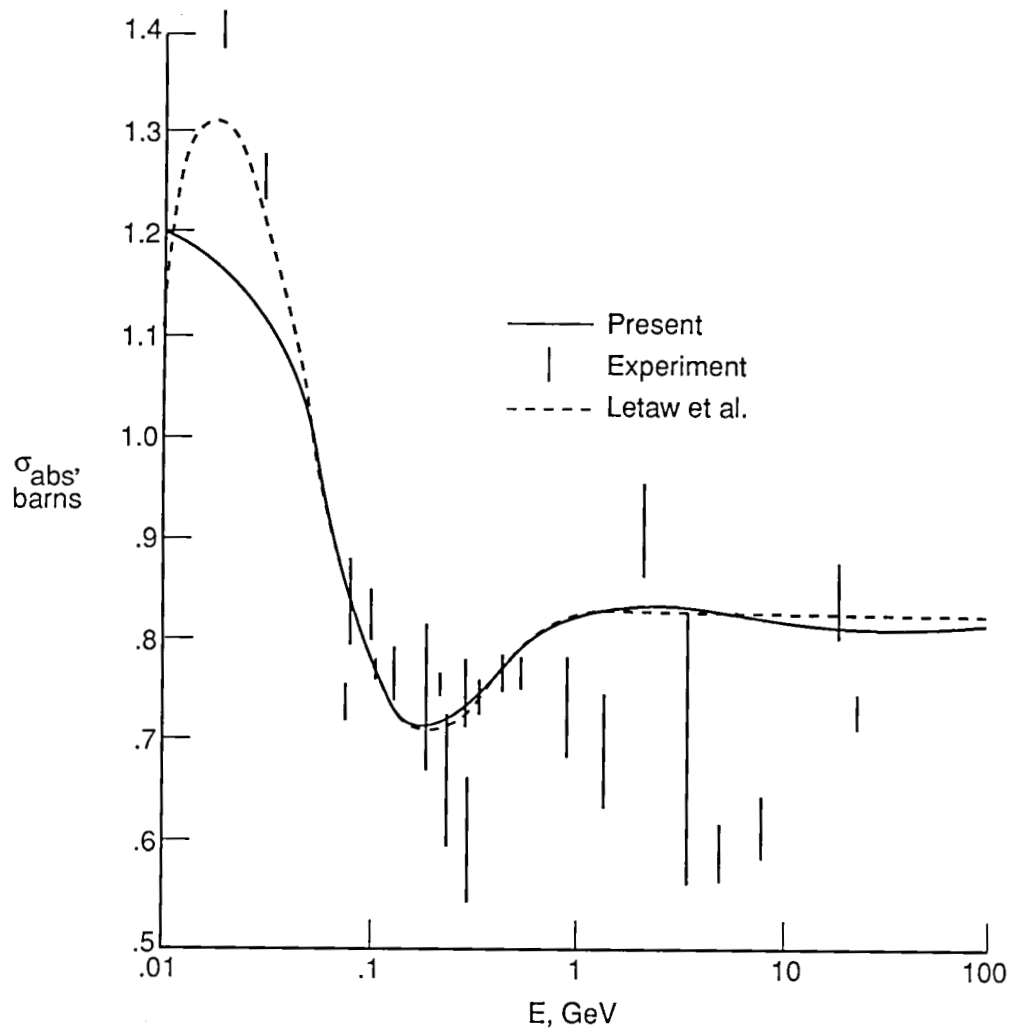
Figure 16. The neutron-copper absorption cross sections according to the present formalism, Letaw et al. (ref. 8), and various experiments.
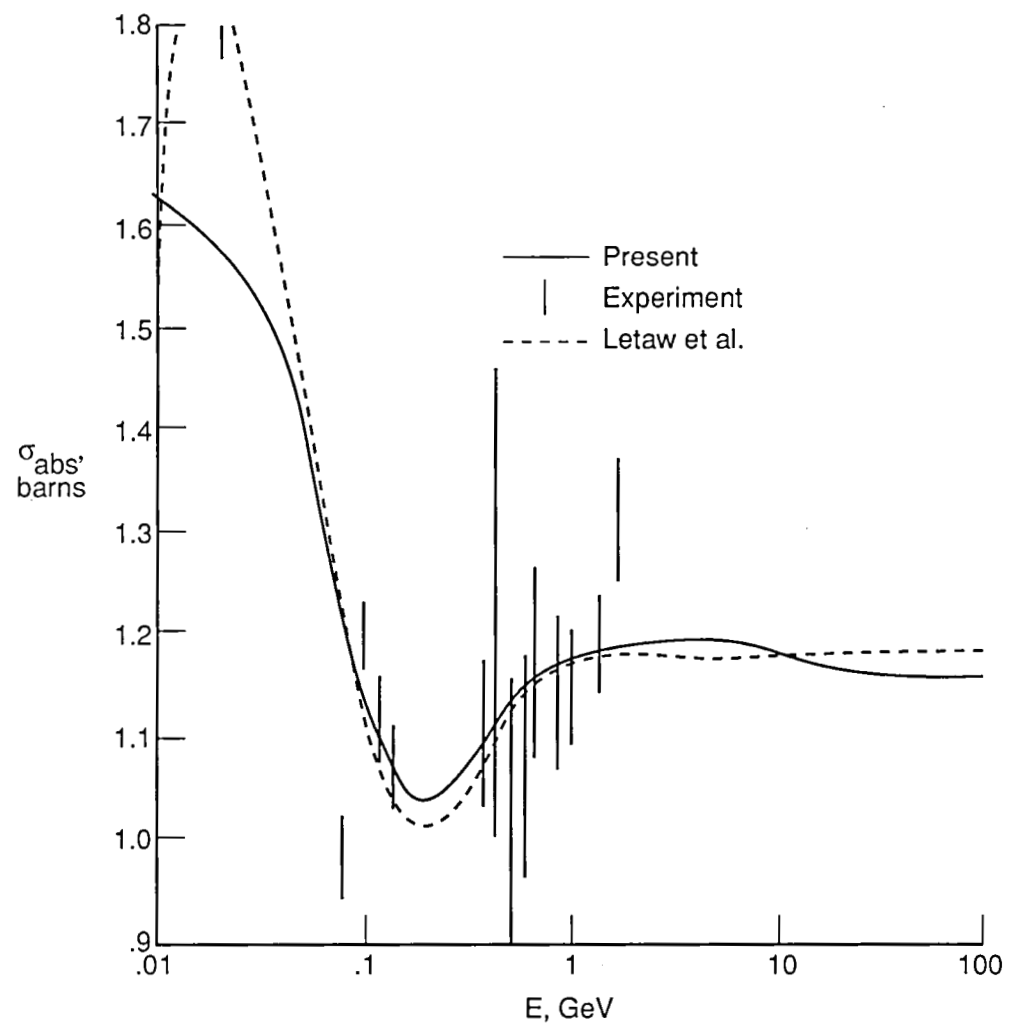
Figure 17. The neutron-silver absorption cross sections according to the present formalism, Letaw et al. (ref. 8), and various experiments.
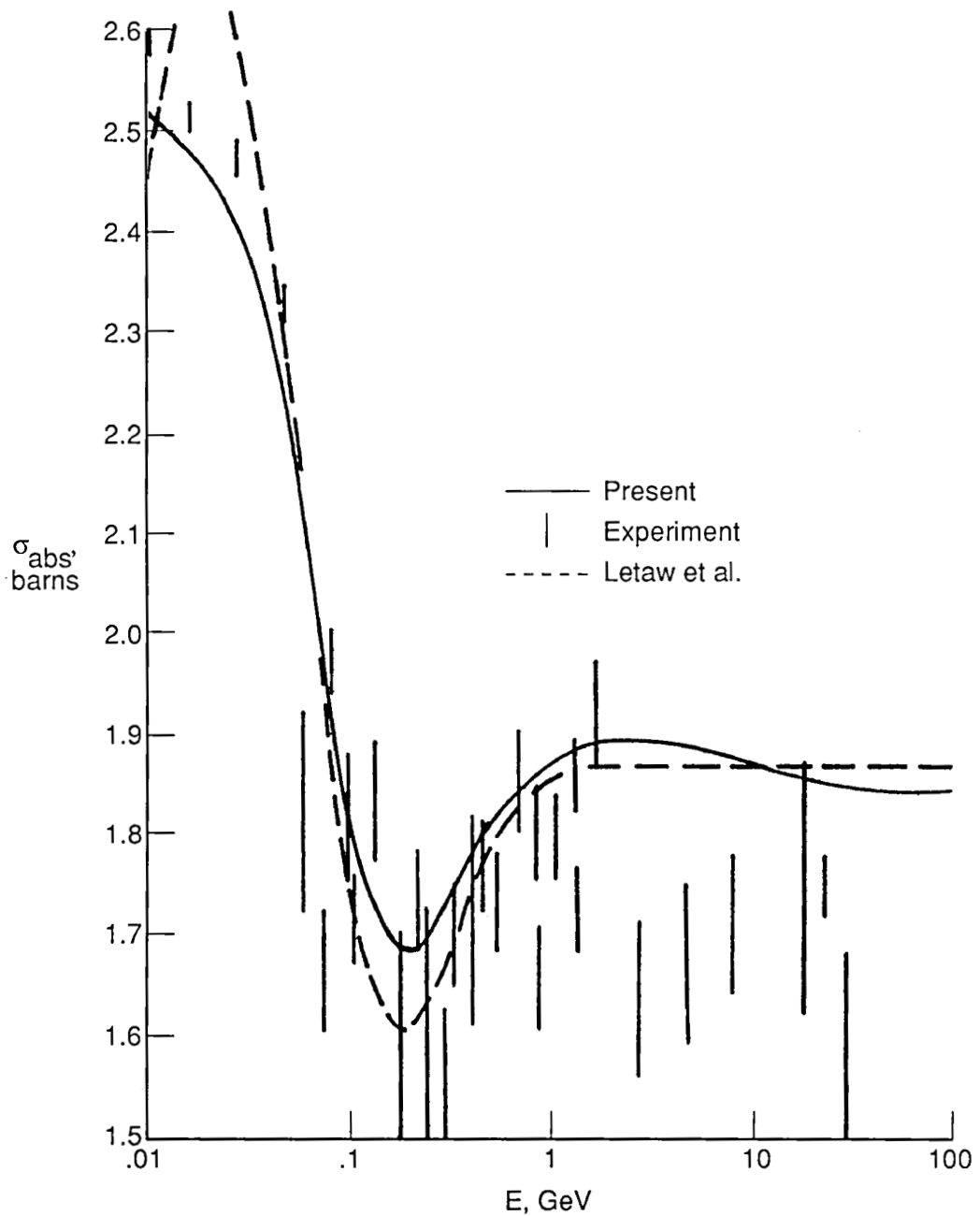
Figure 18. The neutron-lead absorption cross sections according to the present formalism, Letaw et al. (ref. 8), and various experiments.
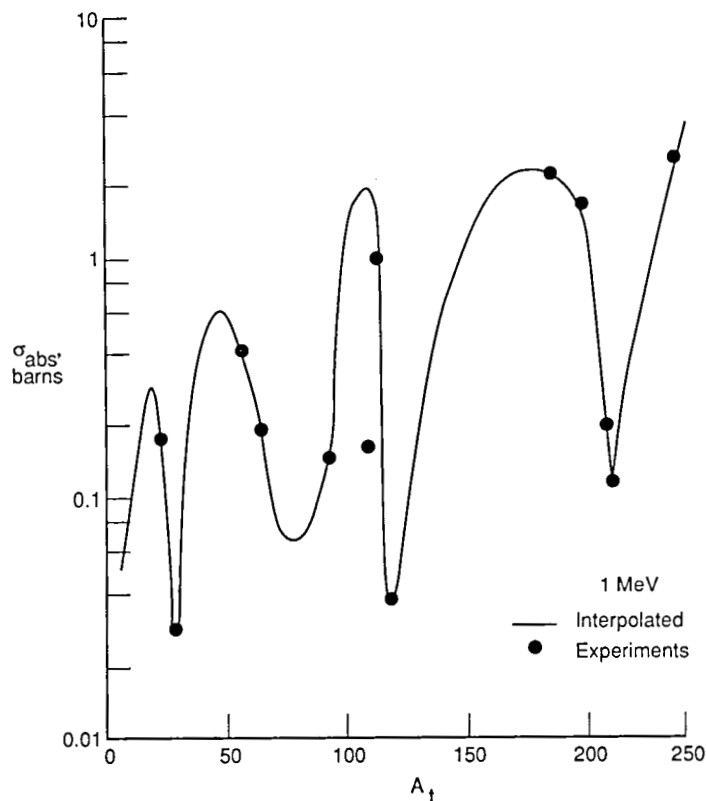
Figure 19. The neutron-nucleus absorption cross sections at 1 MeV of the present formalism and various experiments.
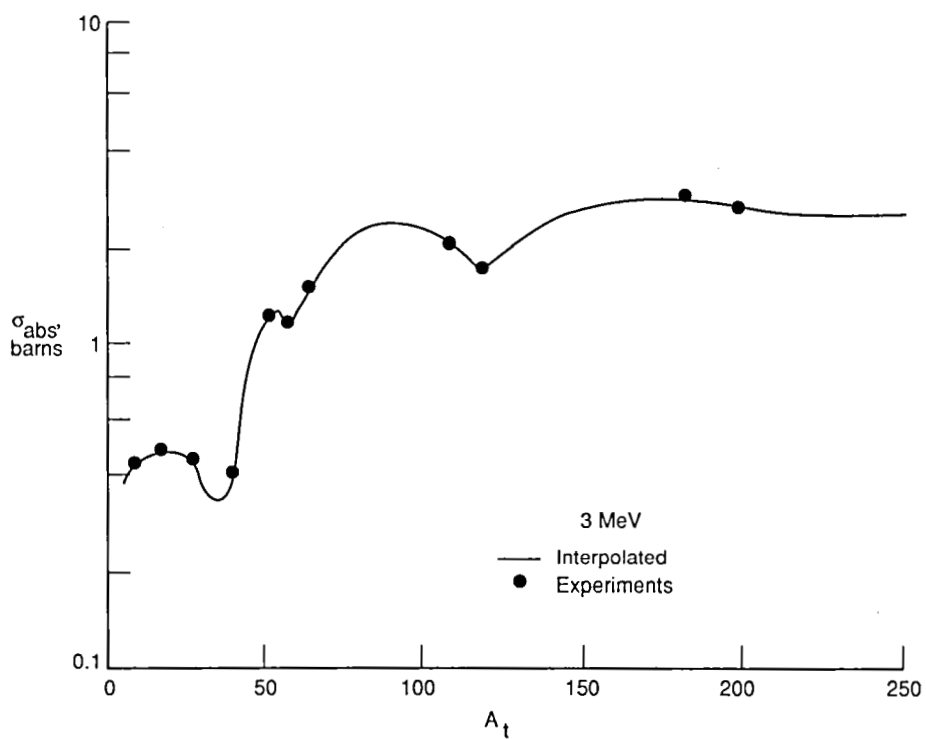
Figure 20. The neutron-nucleus absorption cross sections at 3 MeV of the present formalism and various experiments.
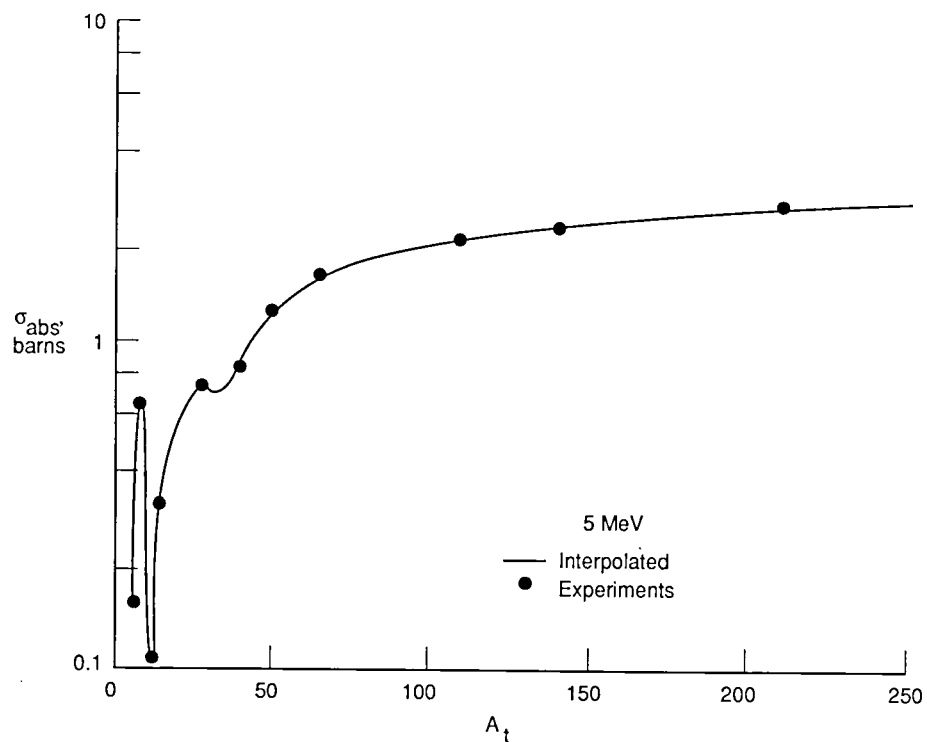
Figure 21. The neutron-nucleus absorption cross sections at 5 MeV of the present formalism and various experiments.
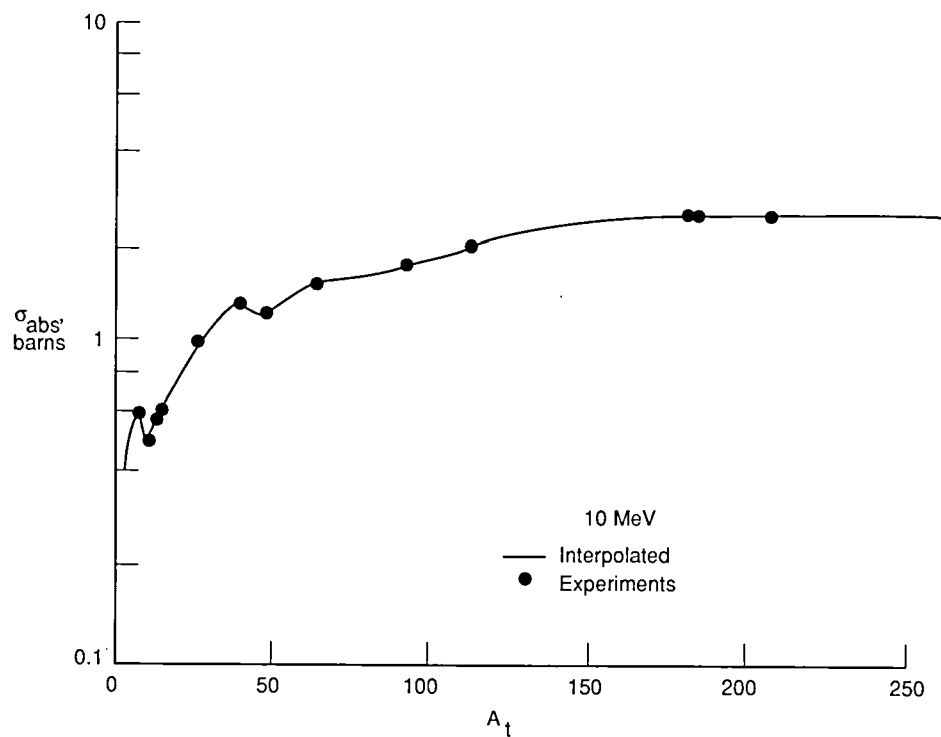

Figure 22. The neutron-nucleus absorption cross sections at 10 MeV of the present formalism and various experiments.
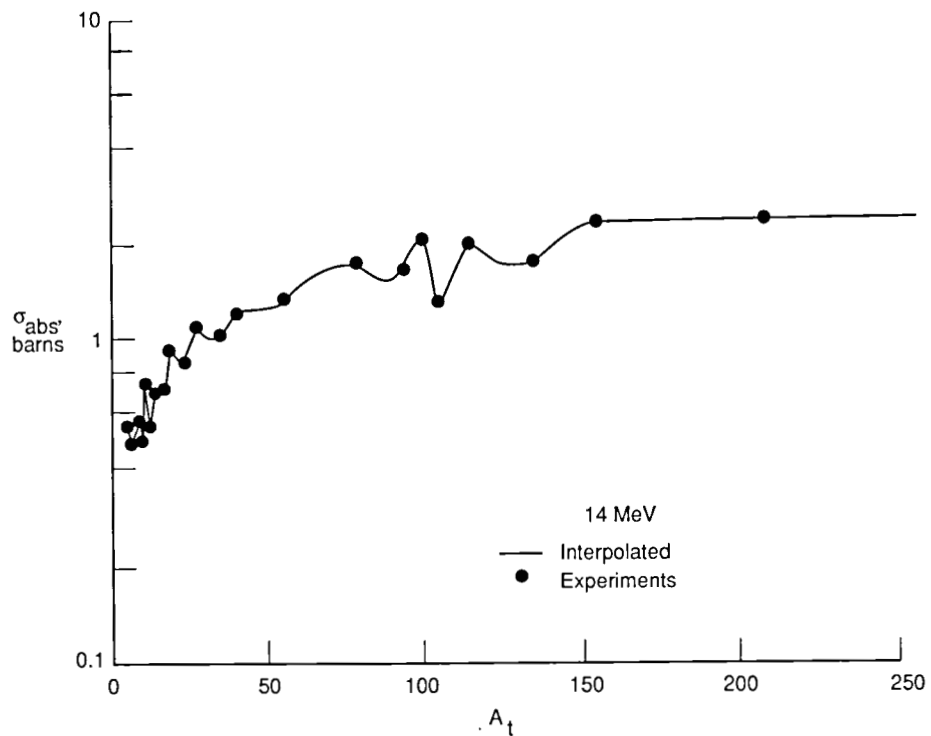
Figure 23. The neutron-nucleus absorption cross sections at 14 MeV of the present formalism and various experiments.
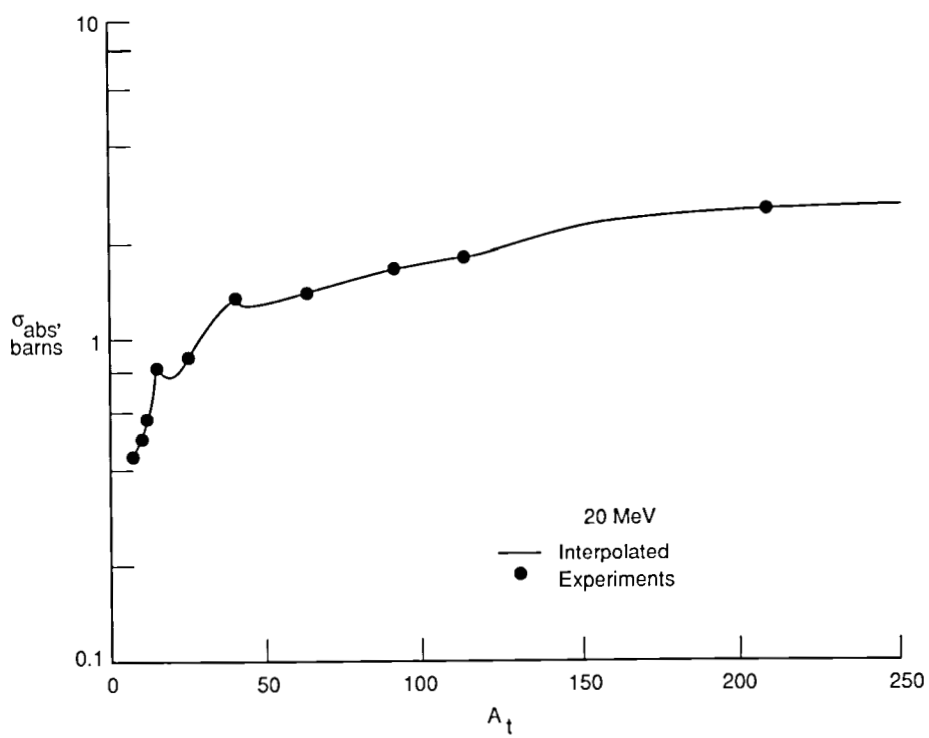

Figure 24. The neutron-nucleus absorption cross sections at 20 MeV of the present formalism and various experiments.
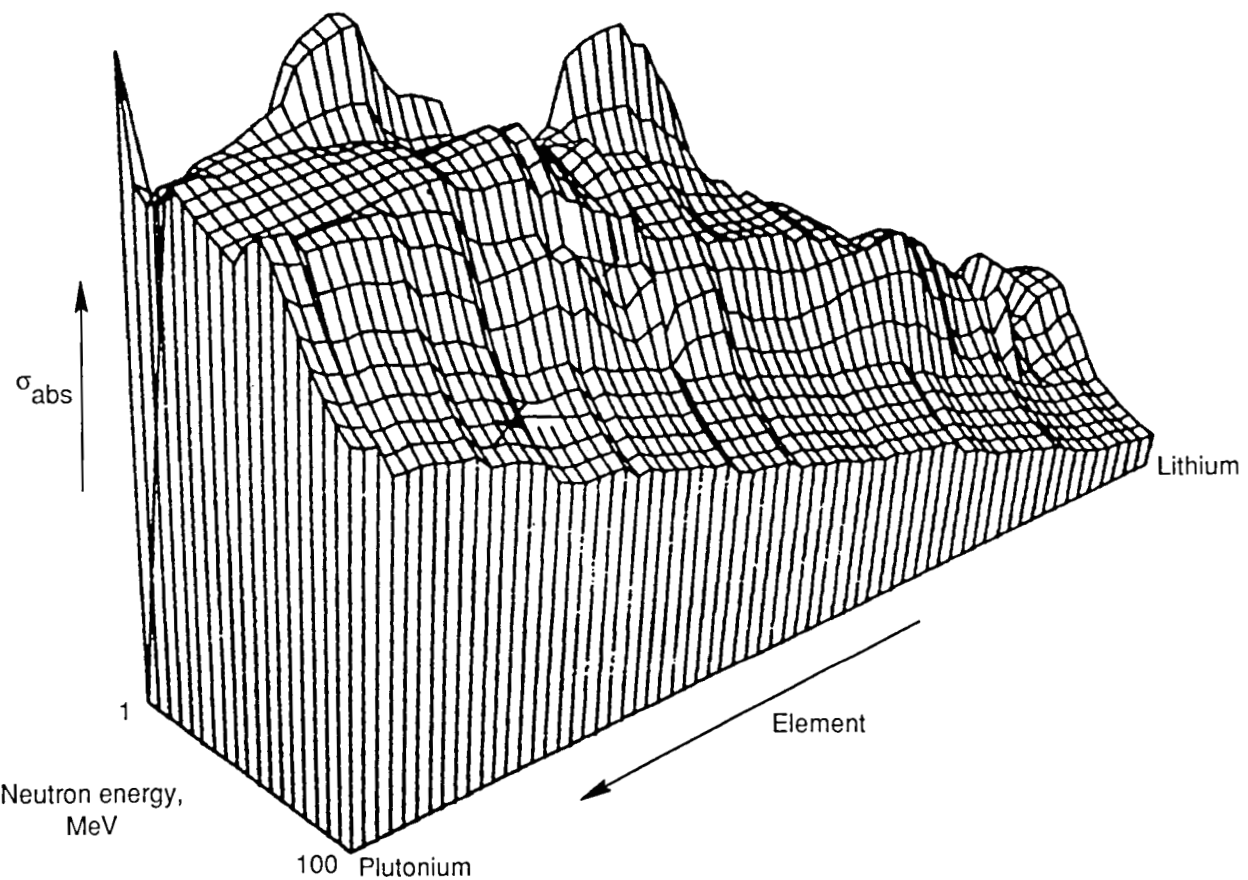
Figure 25. The neutron-nucleus absorption cross sections according to the present formalism.
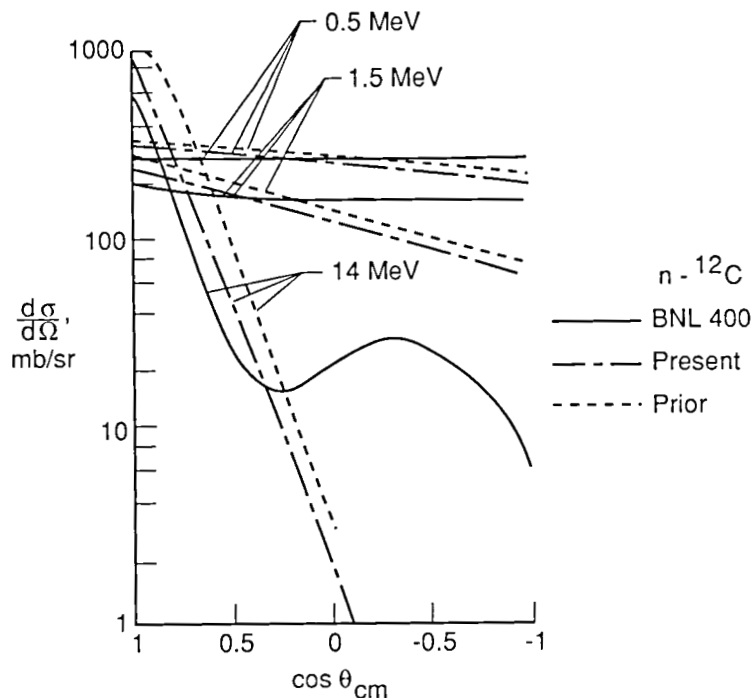
Figure 26. Neutron carbon scattering cross sections according to present formalism, prior formalism (ref. 1), and evaluated data (ref. 15).
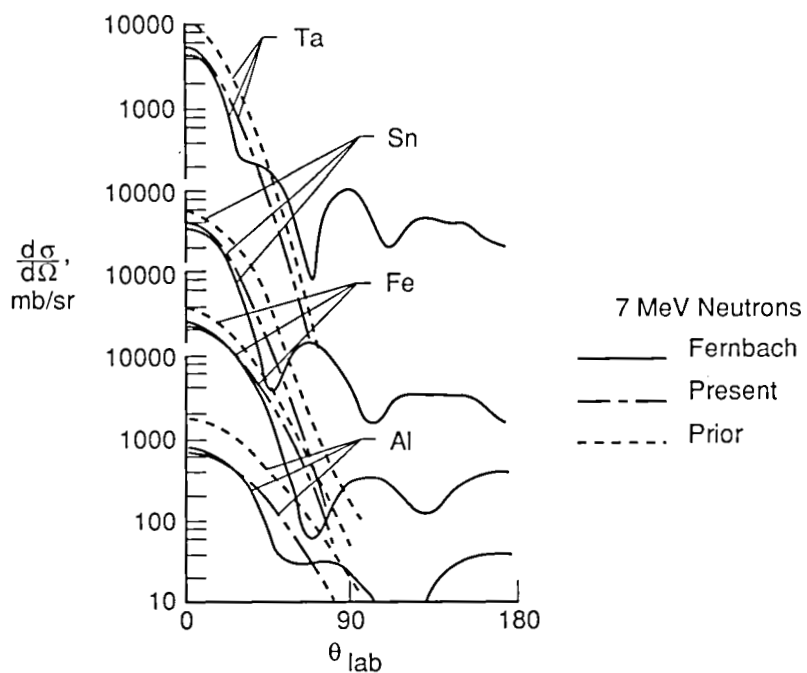

Figure 27. Neutron scattering cross sections for several elements according to present formalism, prior formalism (ref. 1), and the calculations of Fernbach (ref. 14).
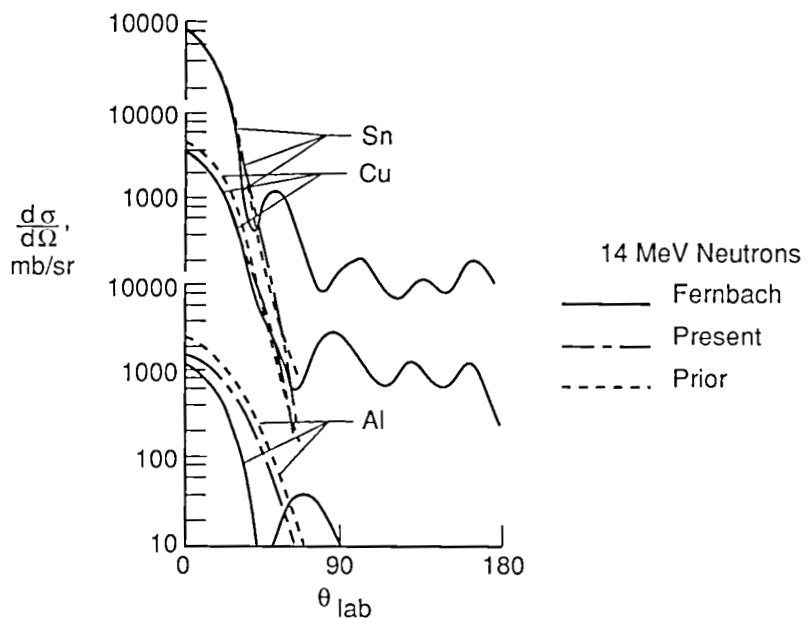
Figure 28. Neutron scattering cross sections for several elements according to present formalism, prior formalism (ref. 1), and the calculations of Fernbach (ref. 14).
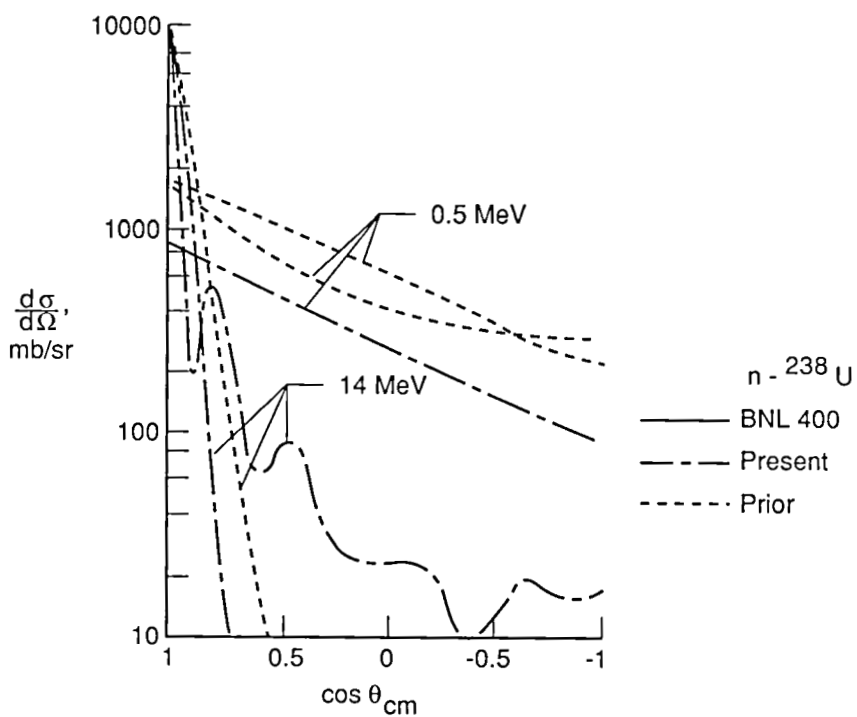

Figure 29. Neutron-uranium scattering cross sections according to present formalism, prior formalism (ref. 1), and evaluated data (ref. 15).

Report Documentation Page

1. Report No. NASA TM-4053	2. Government Accession No.	3. Recipient's Catalog No.
4. Title and Subtitle Nucleon-Nucleus Interaction Data Base: Total Nuclear and Absorption Cross Sections		5. Report Date August 1988
		6. Performing Organization Code
7. Author(s) J. W. Wilson, L. W. Townsend, W. W. Buck, S. Y. Chun, B. S. Hong, and S. L. Lamkin		8. Performing Organization Report No. L-16461
9. Performing Organization Name and Address NASA Langley Research Center Hampton, VA 23665-5225		10. Work Unit No. 199-22-76-01
		11. Contract or Grant No.
12. Sponsoring Agency Name and Address National Aeronautics and Space Administration Washington, DC 20546-0001		13. Type of Report and Period Covered Technical Memorandum
		14. Sponsoring Agency Code

15. Supplementary Notes

    J. W. Wilson and L. W. Townsend: Langley Research Center, Hampton, Virginia.
    W. W. Buck, S. Y. Chun, and B. S. Hong: Hampton University, Hampton, Virginia.
    S. L. Lamkin: Planning Research Corporation, Hampton, Virginia.

16. Abstract

    Neutron total cross sections are represented for Li to Pu targets at energies above 0.1 MeV and less than 100 MeV using a modified nuclear Ramsauer formalism. The formalism is derived for energies above 100 MeV by fitting theoretical cross sections. Neutron absorption cross sections are represented by analytic expressions of similar form, but shape resonance phenomena of the Ramsauer effect are not present. Elastic differential cross sections are given as a renormalized impulse approximation. These cross section data bases will be useful for nucleon transport applications.

17. Key Words (Suggested by Authors(s)) Data bases Neutron-nucleus Cross sections	18. Distribution Statement Unclassified—Unlimited Subject Category 73
19. Security Classif.(of this report) Unclassified	20. Security Classif.(of this page) Unclassified

19. Security Classif.(of this report) Unclassified	20. Security Classif.(of this page) Unclassified	21. No. of Pages 25	22. Price A02

National Aeronautics and
Space Administration
Code NTT-4

Washington, D.C.
20546-0001

NASA

POSTMASTER: If Undeliverable (Section 158
Postal Manual) Do Not Return